A single-crystal neutron diffraction study of NH_4MnF_3

1995 J. Phys.: Condens. Matter 7 563

(http://iopscience.iop.org/0953-8984/7/3/011)

J. Phys.: Condens. Matter 7 (1995) 563–575. Printed in the UK

A single-crystal neutron diffraction study of NH_4MnF_3

J Rubín†‡, E Palacios†, J Bartolomé† and J Rodriguez-Carvajal§‖

† Instituto de Ciencia de Materiales de Aragón, CSIC–Universidad de Zaragoza, 50009 Zaragoza, Spain

‡ Departamento de Física de la Materia Condensada, Facultad de Ciencias, Universidad de Zaragoza, 50009 Zaragoza, Spain

§ Laboratoire Léon Brillouin (CEA-CNRS), CE Saclay, 91191 Gif sur Yvette Cédex, France

‖ Institut Laue-Langevin, 38043 Grenoble Cédex, France

Received 15 August 1994, in final form 11 October 1994

Abstract. Neutron diffraction measurements have been performed on a single crystal of the ammonium perovskite NH_4MnF_3 at 220 K, 80 K and 20 K. This perovskite is known to undergo a transition from cubic ($Pm\bar{3}m$, $Z = 1$) to orthorhombic ($Pnma$, $Z = 4$) structure at $T_c = 182$ K and an antiferromagnetic transition at $T_N = 75$ K. In the cubic phase, the rotational structure factor method has been used to obtain the parameters of the interaction potential of the NH_4^+ molecule with its crystal environment. In the orthorhombic phase, the refinement shows that a single orientation of the NH_4^+ molecule in the crystal is populated. This gives rise to a fully ordered sublattice of NH_4^+ groups related to the distortion of the perovskite and the appearance of two types of hydrogen bond. In the magnetic phase, an antiferromagnetic G_y structure is deduced with a magnetic moment of $3.6(2)\mu_B$.

1. Introduction

Ammonium fluoroperovskites NH_4MF_3 (M = 3d or 4d metal) provide an interesting model system of the dynamics of the NH_4^+ ions, since they have a cubic phase ($Pm\bar{3}m$, $Z = 1$) at high temperature, while they undergo a first-order transition to a lower-symmetry structure upon cooling. Recently, after the resolution of the low-temperature structure of NH_4CdF_3 (Le Bail *et al* 1990) ($Pnma$, $Z = 4$), a new series of studies on these compounds was undertaken with the aim of finding precisely the atomic positions.

The low-temperature structure of NH_4MnF_3 was solved ($Pnma$) and checked by Raman spectroscopy (Laguna *et al* 1993). The motion of the NH_4^+ ion was studied by means of quasielastic neutron scattering (QNS) (Rubín *et al* 1994a), where it was demonstrated that the NH_4^+ ion jumps stochastically between at least two distinguishable and equivalent orientations in the high-temperature phase. An axis of preferential rotation, the C_{2z}, was proposed, i.e. the predominant reorientations were of 180°, and the relative predominance with respect to other axes increased for decreasing temperature. In the low-temperature phase the QNS results could only be explained in terms of an asymmetric double-well potential barrier of unclear origin. The activation energies involved in the rotational process were deduced for both high- and low-temperature phases (Rubín *et al* 1994a). In an inelastic neutron scattering (INS) study (Rubín *et al* 1994b), the excitation energies of the librational motion in the high-and low-temperature phases of NH_4MnF_3 were determined. A rotational potential could be deduced, expressed in terms of symmetry adapted functions, for the high- and the low-temperature phases, for both the Zn and Mn compounds.

0953-8984/95/030563+13$19.50

In spite of this progress, it was deemed interesting to perform a single-crystal neutron diffraction (SCND) study of NH_4MnF_3, since this compound has its structural transition at $T_c = 182$ K (Helmholdt *et al* 1980) and a para- to weak antiferromagnetic transition at $T_N = 85$ K (Bartolomé *et al* 1983). In this sample we wanted to verify the previous results of the low-temperature phase determination done on powder, to determine the positions of the H atoms, impossible to do with x-rays, and determine its magnetic structure. However, there were other motivations: in the high-temperature phase other authors have proposed, from van der Waals energy calculations, the possibility of finding the N–H bond pointing towards the metal atoms in the high-temperature phase (Fayos 1990), quite contrary to our prediction that such an orientation was highly improbable. On the other hand, SCND provides a different method of determining the hindering barrier, taking into account the fact that the orientational disorder of the NH_4^+ ions in the high-temperature phase may be described by means of the neutron scattering rotational structure factor (Press and Hüller 1973). SCND has been applied to related compounds like ND_4Br (Press 1973) or $(NH_4)_2SnCl_6$ (Vogt and Prandl 1983, Brückel *et al* 1984) and some discrepancies were found with respect to the barrier parameters deduced with other techniques. Since we have an independent determination for the barrier (Rubín *et al* 1994b), the present work should allow a further check on the method as well.

In the low-temperature phase (Laguna *et al* 1993), it has been proposed that each NH_4^+ ion is oriented so that there exist four H bonds of type N–H...F with four F atoms, which form a tetrahedral cage, in each pseudocubic cell. Since there are four such tetrahedral cages in the low-temperature distorted structure, the NH_4^+ ions order in four sublattices such that each ion is rotated by 90° or 180° with respect to the adjacent ones. The predictions from van der Waals force calculations (Fayos 1990) propose that the most probable deformation would be the one that favours four single H bonds too. We have the purpose of verifying these two predictions and determining precise N–H distances.

Below $T_N = 75$ K NH_4MnF_3 is known to behave as a weak ferromagnet, as detected from AC susceptibility measurements. However, the magnetization measurements could not detect a canting angle, thus establishing a higher limit for it of 0.1° (Bartolomé *et al* 1983). On the other hand, in the previous powder neutron diffraction work on NH_4MnF_3 and NH_4CoF_3, the appearance of the $\{\frac{1}{2}, \frac{1}{2}, \frac{1}{2}\}$ magnetic reflections (with respect to the pseudocubic reciprocal cell) indicated an antiferromagnetic ordering of G type (Helmholdt *et al* 1980). The present work allows the determination of the direction and magnitude of the magnetic moment of Mn in this compound.

2. Experimental details

The NH_4MnF_3 single crystal on which measurements were made was grown by hydrothermal synthesis, in which a stoichiometric mixture of NH_4HF and MnF_2 was heated up to 673 K for one week under autogenous pressure. The crystal was a prism of $0.8 \times 0.8 \times 1$ mm^3 side size. The crystal was glued to a Displex refrigerator support on one base.

The neutron diffraction experiment was performed on the D9 diffractometer of the high-flux reactor at the Institut Laue–Langevin. The wavelength of the incoming neutrons was $\lambda_0 = 0.8434$ Å, and a bidimensional 32×32 pixel ^{3}He detector was used. For each reflection the integrated intensity was obtained. The experiment was performed at 220 K (209 reflections measured in the first octant $h, k, l \geqslant 0$ and 95 in the second $h < 0, k, l \geqslant 0$), at 80 K (552 reflections measured) and at 20 K (534 reflections). Apparently, the stress due

to the glue was enough to produce a constraint that set the elongation axis perpendicular to the glued base, reduced the number of crystallographic domains and increased their size. To obtain a reasonable quality of the diffracted peaks at low temperatures a moderately low cooling rate (30 K h^{-1}) had to be applied.

3. Structure determination

The NH_4MnF_3 perovskite undergoes a first-order phase transition at $T_c = 182$ K (Burriel *et al* 1984) from cubic to orthorhombic structure (Laguna *et al* 1993). The analysis of the diffraction data is different for the two phases: in the cubic phase there is a high degree of NH_4^+ dynamical orientational disorder, while it reduces drastically below T_c. Then the rotational molecule form factor method may be advantageous in the high-temperature phase since it yields information on the rotational distribution function (see below). On the other hand, in the distorted phase the NH_4^+ ions are ordered, so the hydrogen atoms are strongly localized. This makes unpractical the use of the rotational distribution function. Moreover, the quality of the data in the low-temperature phase is worse and the number of parameters is too high for the above method to be applied. Therefore only the conventional analysis has been used.

3.1. The cubic phase

In the cubic phase the NH_4^+ is located in the centre of the space left by eight MF_6 regular octahedra that share apices. In a first approach the data were treated with the conventional method, proposing 24 sites for H with equal occupation probability. The result of this analysis, given in table 1 ($R_w = 4.85\%$), is in good agreement with a previous powder neutron diffraction study (Helmholdt *et al* 1980). The H atoms deviate slightly from the N–F line. Also the NH_4^+ tetrahedron is not perfect, the angles differing slightly from 109.5°, but the departure from regularity is slightly less than that determined from the powder diffraction study. Also the N–H distance (0.987 Å), is slightly lower than the previous determination (1.03 Å). Note also that the U_{22} for F is four times larger than U_{11} (Mn–F–Mn bond), which is indicative of the oscillatory motion of the MnF_6 octahedra in the M and R phonon modes.

In a second approach the rotational form factor formalism was applied following the notation and method given by Press (1973). The NH_4^+ ion was now considered as a regular tetrahedron in an O_h site symmetry. Because of centrosymmetry, the contribution of the NH_4^+ ion to the structure factor is real and equal to

$$A(Q) = e^{-U^2Q^2/2}\left\{b_N + 4b_H \sum_{L,m} c_{Lm}(-1)^{L/2} j_L(Qr) K_{Lm}(\Omega)\right\} \qquad (1)$$

where $Q = (2\pi/a)(h, k, l)$ is the scattering vector, r is the N–H distance, U is the thermal factor, Ω is the direction of the momentum transfer vector, Q, in polar angles in a coordinate system defined by the crystallographic axes, j_L is the spherical Bessel function of order L, and K_{Lm} are cubic harmonics of order L. For the present symmetry case, only $m = 1$ terms appear for $L < 10$.

Expression (1), added to the amplitude contribution of the Mn and F atoms, has been used as the structure factor to fit the integrated intensities of the experimental Bragg peaks and the quantities c_L have been taken as fit parameters. From the fit it was concluded that

Table 1. Structural data of NH_4MnF_3 in the cubic phase (220 K) obtained with the conventional model. 24 equivalent positions for four H atoms have been assumed. (Standard deviations are in brackets.)

Atom	Mn	F	N	H
Site	1a	3d	1b	24i
x/a	0	$\frac{1}{2}$	$\frac{1}{2}$	$\frac{1}{2}$
y/b	0	0	$\frac{1}{2}$	0.686 92(45)
z/c	0	0	$\frac{1}{2}$	0.638 95(46)
Occupation	1	3	1	4
U_{11} (Å^2)	0.006 52(17)	0.006 15(28)	0.014 52(14)	0.039 28(09)
U_{22}	U_{11}	0.025 89(28)	U_{11}	0.048 25(60)
U_{33}	U_{11}	U_{22}	U_{11}	0.040 07(38)
U_{12}	0	0	0	0
U_{13}	0	0	0	0
U_{23}	0	0	0	−0.018 49(47)

Weighted R factor: $R_w = 4.85\%$

$a = 4.2364(4)$ Å[a]	Angle(H–N–H) = 110.85(30)°[b]
N–H = 0.9866(27) Å	Angle(H–N–H) = 106.74(17)°[c]

[a] As obtained from powder diffraction for $T = 220$ K (Helmholdt *et al* 1980).
[b] Both H in a $\frac{1}{2}, y, z$ plane.
[c] One H in a $\frac{1}{2}, y, z$ plane and one in a $y, \frac{1}{2}, z$ plane.

the series could be truncated at $L = 8$ since this term only contributes at most 1% of the structure factor $A(Q)$ in the Q region scanned in this experiment.

Once the c_L have been determined from experiment, it is possible to derive the hindering potential taking into account the following relations. The coefficients

$$c_L = \frac{8\pi^2}{2L+1}\sqrt{4\pi}M_L\Pi_L \tag{2}$$

enter into the definition of the rotational distribution function

$$f(\omega) = \sum_L M_L H_L(\omega) \tag{3}$$

through the M_L constants. $H_L(\omega)$ are cubic rotator functions and ω the Euler angles defining the orientation of the NH_4^+ ion with respect to the crystallographic axes. The cubic rotator functions are symmetry adapted functions that form a complete set of orthogonal functions with the symmetry of both the crystal (point group O_h) and the rotor (the tetrahedral NH_4^+ ion, point group T_d). The Π_L constants depend only on the form of the molecule, and for a regular tetrahedron

$$\Pi_0 = \frac{1}{\sqrt{4\pi}} \qquad \Pi_3 = \frac{1}{\sqrt{4\pi}}\frac{1}{3}\sqrt{5\times 7} \qquad \Pi_4 = -\frac{1}{\sqrt{4\pi}}\sqrt{\frac{7}{3}}$$
$$\Pi_6 = \frac{1}{\sqrt{4\pi}}\frac{4}{9}\sqrt{2\times 13} \qquad \Pi_8 = \frac{1}{\sqrt{4\pi}}\frac{1}{9}\sqrt{\frac{11\times 17}{3}}. \tag{4}$$

On the other hand, in the classical stochastical limit applicable in the range of temperatures involved ($T > 200$ K), the rotational distribution function may be expressed as

$$f(\omega) = (1/Z)\mathrm{e}^{-V(\omega)/kT} \tag{5}$$

with

$$Z = \int_{\text{sphere}} e^{-V(\omega)/kT}\, d\omega$$

where $V(\omega)$ is the hindering barrier to rotation, which may be expressed in terms of cubic rotator functions truncated at sixth order (Bartolomé *et al* 1977)

$$V(\omega) = A_4 H_4(\omega) + A_6 H_6(\omega). \tag{6}$$

If one identifies (3) and (5), multiplies both members by $H_L(\omega)$ and integrates over the sphere one obtains the relation

$$M_L = \frac{[(2L+1)/8\pi^2]}{Z} \int_{\text{sphere}} H_L(\omega) e^{-V(\omega)/kT}\, d\omega. \tag{7}$$

By solving (2) numerically, where M_L are given by (7) and $V(\omega)$ is written as (6), the parameters of the potential function, A_4 and A_6, are obtained. The fitting process has been performed with the computer program UPALS (Lundgren 1978), to which subroutines implementing the calculation of Bessel functions, cubic harmonics and the derivatives of the structure factor with respect to c_L and r were added.

The structural data obtained with this treatment are collected in table 2. To be noted is the N–H distance, which agrees within 1% with the determination obtained with the conventional method. This small discrepancy originates from the assumption that the NH_4^+ is a regular tetrahedron in the rotational form factor method, while from the conventional analysis, but also from Raman measurements (Bartolomé *et al* 1985), it is known to be slightly distorted.

Table 2. Structural data of NH_4MnF_3 in the cubic phase (220 K) obtained with the rotational structure factor method (standard deviations in brackets). c_L are the form factor coefficients. A_J are the coefficients of the hindering barrier in terms of cubic rotator functions. $V(\omega) = A_4 H_4(\omega) + A_6 H_6(\omega)$.

	Mn	F	N
Site	1a	3d	1b
x/a	0	$\frac{1}{2}$	$\frac{1}{2}$
y/b	0	0	$\frac{1}{2}$
z/c	0	0	$\frac{1}{2}$
Occupation	1	3	1
U_{11} (Å^2)	0.006 13(75)	0.006 4(12)	0.015 66(60)
U_{22}	U_{11}	0.024 61(11)	U_{11}
U_{33}	U_{11}	U_{22}	U_{11}
U_{12}	0	0	0
U_{13}	0	0	0
U_{23}	0	0	0
r(N–H) = 0.9956(11) Å			
$c_4 = -0.1826(77)$		$A_4 = -319(39)$ K	
$c_6 = -1.035(12)$		$A_6 = 1367(107)$ K	
$c_8 = 0.33(2)$			
$R_w = 5.5\%$			

To compare better the resulting hindering barrier to different theoretical and experimental determinations, it will be expressed in terms of the rotational constant $B = \hbar^2/2I$, where I is the moment of inertia of the NH_4^+ ion, considered as a spherical top (Bartolomé *et al* 1977)

$$V(\omega) = B\beta\{\beta_4 V_4(\omega) + \beta_6 V_6(\omega)\}$$

where β, β_4 and β_6 are dimensionless constants and $\beta_4^2 + \beta_6^2 = 1$. The relation with the A_L constants is $A_4 = 3B\beta\beta_4$ and $A_6 = \sqrt{(13)}B\beta\beta_6$. The values obtained with the N–H distance determined in this work are given in table 3, where all previous determinations have been included. The values of $\beta = 44(4)$, $\beta_4 = -0.27(3)$ and $\beta_6 = 0.963(8)$ correspond to a hindering potential with six distinguishable equivalent orientations, each corresponding to the four protons pointing towards F atoms at mid-edges of the cube; i.e. there are four single H bonds in this orientation. We conclude that this result, together with the QNS work (Rubín *et al* 1994a), solves the question on the most probable orientations of the NH_4^+ ion: it is the so-called four-single-H-bond type, 4SHB (Fayos 1990).

Table 3. A comparison of the hindering barrier parameters β, β_4 and β_6 for NH_4MnF_3 in its high-temperature phase from different theoretical and experimental sources. In references a and b, N–H = 1.04 Å, yielding the given values of B, while in the present work (rotational form factor method) it has been determined as N–H = 0.9956 Å, thus modifying B.

	Theory		Experimental	
Potential parameters	Electrostatic[a]	Buckingham atom–atom[b]	INS[c]	ND (this work)
B (K)	8.48	8.48	9.11	9.11
β	32.52	21.7	50(5)	44(4)
β_4	−0.263	0.106	−0.27(3)	−0.27(3)
β_6	0.965	0.986	0.963(8)	0.963(8)
β_8		−0.051		

[a] Navarro *et al* 1987.
[b] Smith 1987.
[c] Rubín *et al* 1994b.

That the orientation of minimum energy is dominated by the β_6 term in the fluoroperovskites is common to all theoretical and experimental determinations. On the other hand, the ratio β_4/β_6 hardly differs from that derived from the electrostatic model used to interpret heat capacity experiments (Bartolomé *et al* 1977, Navarro *et al* 1987), but differs qualitatively with respect to that predicted with the Buckingham atom–atom potential since the sign is opposite.

We may compare these results to the parameters from the experimental determination by inelastic neutron scattering (INS), which establish that the first librational excited state is 39 meV (Rubín *et al* 1994b). The β_4/β_6 ratio is fixed to the same value as obtained by single-crystal neutron diffraction (SCND) and the scaling factor β is then the fit parameter, yielding the value $\beta = 50(5)$, somewhat higher, but within the experimental error, than the value determined in the present work. In contrast, the discrepancy with respect to the Buckingham model prediction ($\beta = 21.7$) is a factor of two, proving that this latter type of estimation is, at present, unreliable.

The conclusion is that the β values proposed in this work give a reasonable parametrization of the hindering barrier. The angular dependence of the hindering barrier is

well modelled by the simple electrostatic potential, but the barrier height is underestimated by 10%, thus the electrostatic model predicts a too-low barrier height.

A similar verification of the rotational potential parameter values determined with the different techniques (heat capacity, INS and ND) has been done for $(NH_4)_2SnCl_6$ (Brückel *et al* 1984). The conclusions given there were that the parameters obtained from the heat capacity were poor (Smith 1979), while those derived from INS data of librational and tunnelling frequencies (Müller and Hüller 1982) gave a reasonable account of the expectation values $\langle M_L \rangle$ determined from neutron diffraction for temperatures above 100 K. On the other hand, the tunnelling frequencies calculated with the parameters obtained from diffraction (Vogt and Prandl 1983), and using the pocket state formalism, gave a bad account (a discrepancy by a factor of two) of the tunnelling splitting (Brückel *et al* 1984). With all the available information on this compound, a very good reproduction of the parameters deduced from ND was achieved with the Buckingham atom–atom potential (Smith 1985).

In fluoroperovskites the tunnelling splittings were estimated from proton–lattice relaxation with NMR (Palacios *et al* 1989). Though it was not possible to do this for NH_4MnF_3, from the values for NH_4ZnF_3 ($\omega_t = 8.5 \times 10^6$ s^{-1}) and for NH_4CdF_3 ($\omega_t = 5 \times 10^5$ s^{-1}) one may estimate an approximate value ($\omega_t \approx 10^5$ s^{-1}) for the Mn compound, i.e., too small for INS detection. Consequently, our parameters deduced from INS data only reflect the activation energy and the librational frequency, not the tunnelling splitting. This implies a certain lack of information on the overlap of the rotational wavefunctions. In spite of this, there is a reasonable agreement in the scaling factor β. The essential conclusion is identical to that above for the $(NH_4)_2SnCl_6$ compound: both INS and diffraction experiments are necessary to reliably determine the hindering barrier potential. Concerning the large discrepancy of the parameters calculated with the Buckingham model by Smith (1985), we think this is due to insufficient information to determine a too-large number of parameters used to obtain the hindering barrier.

3.2. The orthorhombic phase

In the previous x-ray powder diffraction work (Laguna *et al* 1993) NH_4MnF_3 was determined to be orthorhombic in the low-temperature phase (*Pnma*, $Z = 4$), with $a = 5.952(1)$ Å, $b = 8.543(1)$ Å and $c = 5.949(1)$ Å. This structure may be described as constituted by regular octahedral MF_6 groups, which have tilted at the transition temperature around the three cubic phase axes (to be called pseudocubic axes, x_c, y_c, z_c at $T < T_c$). The octahedra tilt in phase with respect to the y_c axis, [0, 1, 0], by 4.7° (the rotation transforming as the M_{2y} irreducible representation of the cubic first Brillouin zone), and antiphase with respect to the x_c and z_c axes, [1, 0, 0] and [0, 0, 1], by identical angles of 2.4°. However, the proposition of having the NH_4^+ ion in an ordered, oriented state pointing towards the set of four F atoms that form a cage of minimal N–F distances in the pseudocube had been proposed in the study of NH_4CdF_3 (Le Bail *et al* 1990), and in the x-ray and Raman work on NH_4MnF_3 (Laguna *et al* 1993) it was found to be compatible with all the data. As regards the NH_4^+ ion, it was considered as an N atom of refinable occupancy to simulate the effect of the charge distribution of the protons. However, the proposed position of the protons remained to be proved by the present SCND study.

At the temperature of the measurement, $T = 80$ K, it was obvious from the shape of the diffraction spots that the sample was twinned, i.e. it became divided into structural domains of orthorhombic symmetry. This is, of course, a well known effect caused by the similarity of the a and c dimensions of this structure, and poses an additional problem to its resolution.

The following hypotheses were set for the refinement of the diffraction intensities.

(i) The *Pnma* group, $Z = 4$ is assumed.

(ii) The NH_4^+ ion is allowed to populate six different orientations in the pseudocubic cage. This can be described by either different H atomic positions. The population of the six orientations is denominated s_i, $i = 1$–6, definite positive and fulfilling the condition $\sum_{i=1,6} s_i = 1$ ($s_2 = s_3$ as a consequence of the mirror plane in *Pnma*). With the previous assumption one finds eight symmetry independent H positions, with occupation probability p_k, $k = 1$–8, such that

$$p_1 = 4(s_1 + s_4) \qquad p_2 = 4(s_5 + s_6) \qquad p_3 = 4(s_1 + s_6) \qquad p_4 = 4(s_4 + s_5)$$

$$p_5 = 8(s_2 + s_4) \qquad p_6 = 8(s_2 + s_5) \qquad p_7 = 8(s_2 + s_6) \qquad p_8 = 8(s_1 + s_2).$$

(iii) The possible twinned structures are assumed to be such that six types of domain may be formed (the ratio of the orders of the respective point groups of the space groups in the high- and low-temperature phases), each particular domain having its local axes as a permutation of a, b and c. The volume fraction of each domain type in the diffraction beam is denominated m_j, $j = 1$–6, with m_j definite positive and $\sum_{j=1}^{6} m_j = 1$.

With these constraints, the 552 reflections (283 independent, their intensity I such that $I > 5\sigma$; σ = standard deviation) are taken into the refinement, which had 49 variables. The results are given in table 4. It is important to note that the slow cooling rate has yielded a domain structure consisting of just two types of domain, with the b axis perpendicular and antiperpendicular to the single-crystal base, which was glued to the sample holder. Since the overall transition essentially amounts to an elongation along this direction, it seems that the stress induced by the glue, blocking the expansion sideways, produced the beneficial effect of selecting a privileged direction of deformation; this is reflected by the non-zero values of m_1 and m_2, while the other four domains were negligible, or not present. The overall quality of the fit is better than that obtained in the x-ray powder diffraction study.

The next clear conclusion is that only the s_1 orientation is populated, so the rotational motion is frozen, and the NH_4^+ groups form a sublattice of completely oriented molecules. Then, the positions of the H atoms effectively correspond to this orientation, which is precisely that proposed in our previous paper (Laguna *et al* 1993) and also agrees with the 4SHB orientation proposed from energy considerations (Fayos 1990). The symmetry of the site where the NH_4^+ ion is located is C_s (figure 1), the molecule being oriented with two of the H atoms contained in the σ_h plane (H1 and H3) pointing to the F2 atoms labelled F_9 and F_{10}, while the other two, which are symmetric with respect to that plane, point towards the two nearest F1 atoms, labelled F_4 and F_6. These four F atoms form a distorted tetrahedral cage, which houses the NH_4^+ tetrahedron.

The N–H distance ranges between 1.079 Å and 0.973 Å. Therefore, through the distortion, two of the distances have become longer than in the cubic phase while two remain the same, within the experimental errors. This agrees with the previous estimation of an average ⟨N–H⟩ = 1.036 Å deduced at low temperature in the previous ND study (Helmholdt *et al* 1980). The H–N–H angles, ranging between 108° and 113°, correspond, indeed, to a deformed tetrahedron, but are very similar to the results of the cubic phase with the conventional analysis. The distortion of the lattice at the phase transition seems to affect essentially the lengths of the N–H bonds, besides freezing the NH_4^+ lattice dynamics into an ordered structure. The three-dimensional arrangement of the ordered NH_4^+ ions is easily visualized by considering the tetrahedral cages in the complete structure (figure 2). Each NH_4^+ tetrahedron has six nearest-neighbouring NH_4^+ ions, of which the four contained in the a–c plane are rotated by 90° around the b axis, and the two belonging to the adjacent layers

Table 4. Crystallographic data of NH_4MnF_3 at 80 K. Space group *Pnma*, $Z = 4$, with $a = 5.952(1)$ Å, $b = 8.543(1)$ Å and $c = 5.949(1)$ Å (Laguna *et al* 1993). Top section: the best set of parameters. The atom N is actually in a general position $x\frac{1}{4}z$. However, the initial fits gave $x \approx 0.5$ and $z \approx 0$ with large standard deviations (as much as the deviation from $x = 0.5$ and $z = 0$), and consequently these latter values were fixed in the final fit. The isotropic thermal parameter is used for Mn, while for the other atoms anisotropic thermal parameters are used (the average of the eigenvalues of the diagonalized matrix of thermal parameters is given for the N, F atoms and the occupied H atoms). Bottom section: Hk, $k = 1, \ldots, 8$, are the non-equivalent possible sites for the H atoms, m_1 and m_2 describe the volume fraction of the domains with the b axis aligned perpendicular and antiperpendicular to the face of the crystal, which was glued to the sample holder, and s_i describe the probability of each of the six orientations of the NH_4^+ ion with four single H bonds. $R_w = 6.1\%$, $R = 7.1\%$ (considering all reflections).

Atom	Position	x/a	y/b	z/c	Occupation	$\langle U \rangle$ (Å^2)
Mn	4a	0	0	0	4	0.0167(15)
N	4c	0.5000	$\frac{1}{4}$	0.0000	4	0.017
F1	8d	0.2718(16)	0.0069(18)	0.7692(22)	8	0.020
F2	4c	−0.0152(37)	$\frac{1}{4}$	0.0210(29)	4	0.021
H1	4c	−0.0365(38)	$\frac{1}{4}$	0.3405(49)	3.85(22)	0.026
H2	4c	−0.0075	$\frac{1}{4}$	0.6722	0.20(18)	
H3	4c	0.1691(61)	$\frac{1}{4}$	0.5138(67)	4.05(23)	0.085
H4	4c	−0.1723	$\frac{1}{4}$	0.4966	0.00(15)	
H5	8d	0.0927	0.1693	0.5930	0.00(25)	
H6	8d	0.0595	0.1608	0.4370	0.00(26)	
H7	8d	−0.0878	0.3355	0.4120	0.40(27)	
H8	8d	−0.0644(29)	0.3551(18)	0.5771(22)	7.70(44)	0.053

	N–F (Å)	N–H (Å)	H–N–H angles (°)
$m_1 = 0.683(25)$	N–F_1 = 3.081(14)	N–H1 = 0.973(29)	H1–N–H3 = 107.6(58)
$m_2 = 0.317(25)$	N–F_2 = 2.924(14)	N–H3 = 1.010(36)	H1–N–H8 = 109.6(38)
$s_1 = 0.962(52)$	N–F_3 = 3.162(14)	N–H8 = 1.079(15)	H3–N–H8 = 108.6(45)
$s_2 = 0.000(21)$	N–F_4 = 2.836(14)		H8–N–H8 = 112.7(27)
$s_3 = s_2$	N–F_5 = 3.162(14)		
$s_4 = 0.000(33)$	N–F_6 = 2.836(14)		
$s_5 = 0.000(28)$	N–F_7 = 3.081(14)		
$s_6 = 0.050(39)$	N–F_8 = 2.924(14)		
	N–F_9 = 2.851(17)		
	N–F_{10} = 2.888(22)		
	N–F_{11} = 3.101(17)		
	N–F_{12} = 3.073(22)		

$\langle$Mn–F$\rangle$ = 2.122(12) Å

are rotated by 180°; this forms four interpenetrating sublattices, i.e. an antiferrodistortive ordered structure.

Regarding the H bond strength, one notices that the F1 atoms are exclusively bound to an H atom (labelled H8) of one NH_4^+ ion (position A in figure 2), and are correlated with the longest N–H distance, that is, the H...F bond is enhanced and the N–H bond weakened. On the other hand, each F2 atom caters for two inequivalent hydrogen atoms (labelled H1 and H3, and position B in figure 2), each belonging to two different NH_4^+ ions. The corresponding N–F distance is longer and the N–H distance shorter. Consequently, there are three different F...H bonds, which can be classified into two types: two H atoms (H8, equivalent by symmetry) of the NH_4^+ molecule with the strongest H bonds (type A) and the other two H atoms (H1 and H3) with weaker and different H bonds (type B).

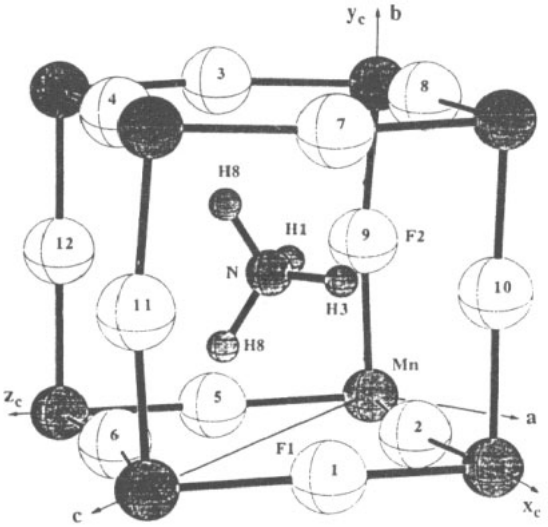

Figure 1. The surrounding atoms of the NH_4^+ ion in the orthorhombic structure of NH_4MnF_3. The NH_4^+ ion is located in a site of C_s symmetry. The twelve F atoms surrounding an NH_4^+ ion have been labelled from 1 to 12. Atoms F_4 and F_6 show the shortest distance to N and the N–H8 distance of the bonds pointing to these atoms is largest. The atoms F_9 and F_{10} attract the other two H atoms.

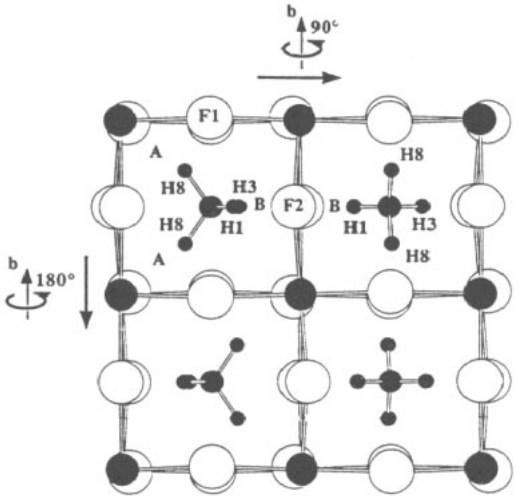

Figure 2. Four adjacent pseudocubic cells showing the four different orientations of the NH_4^+ ions along the *b* axis. Each orientation can be obtained from the others through 90° or 180° rotations around the *b* axis, as indicated by the arrows.

The existence of these three different H bonds was first proposed by Knop *et al* (1981) from infrared spectroscopy of NH_3D^+ species doping the NH_4^+ perovskites. In fact, the stretching mode ν_1(N–D) was split in three bands of relative intensities 1:1:2, which should correspond to three different D...F bonds, and the band of double intensity would correspond to two H atoms related by a mirror plane. We have now determined the crystallographic positions of the atoms involved in these H bonds, the resulting ordered structure that emerges from the arrangement of the NH_4^+ molecule with such bonds and the

correlation between the H bond strength and the type of F atom.

4. The magnetic structure

It is known that below $T_N = 75$ K the magnetic moments of Mn in NH_4MnF_3 are ordered (Bartolomé *et al* 1983) with a magnetic structure of type G, as determined by powder neutron diffraction (Helmholdt *et al* 1980). Our single-crystal data taken at 20 K is used to determine the direction and magnitude of the magnetic moment. The quality of the reflections measured at 20 K is similar to the data collected at 80 K.

A qualitative analysis of the magnetic structure is performed on the difference between the 20 K and the 80 K reflections, since only at 20 K are there magnetic contributions. It should be noted that *hkl* and *lkh* reflections overlap because of twinning, and therefore the observed reflections are not pure magnetic ones, i.e. with extinction of the nuclear part of the structure factor. However, the 20 K − 80 K reflections give an estimation of the magnetic contribution below T_N, but they are not direct measurements of the magnetic contribution, since the positional and thermal parameters and domain structure are different at both temperatures. In table 5 we have collected the reflections that show the largest difference of intensity between the two sets of data.

Table 5. The magnetic reflections deduced from the difference $I_{exp} = I_{hkl}(20\ K) - I_{hkl}(80\ K)$ normalized to I_{exp} of reflection (011), which is given the value 100 conventionally. No is the code number of the peak, *hkl* are the Miller indices, and I_{calc} are the calculated intensities for the G_y structure and G_x structure. The intensities of the G_z structure are the same as those of G_x, but switching h and l. $\langle I_{cal}(G_x)\rangle$ is the average of the intensities of the reflections *hkl* and *lkh*.

No	h	k	l	I_{exp}	$\langle I_{exp}\rangle$	$I_{calc}(G_y)$	$I_{calc}(G_x)$	$\langle I_{calc}(G_x)\rangle$
1	0	1	1	100	100.09	155.00	230.4	152.76
	1	1	0	100.17			75.11	
2	0	3	1	43.82	36.80	12.25	68.6	62.25
	1	3	0	29.77			55.9	
3	1	1	2	64.58	62.39	60.98	54.63	36.40
	2	1	1	60.20			18.16	
4	1	3	2	33.75	33.46	16.13	26.97	22.16
	2	3	1	33.16			17.35	
5	0	1	3	34.23	41.10	28.14	29.50	15.51
	3	1	0	47.96			1.52	
6	0	5	1	10.59	12.80	1.20	15.81	15.21
	1	5	0	15.00			14.61	
7	0	3	3	23.05	21.78	10.27	15.20	10.1
	3	3	0	20.51			5.00	
8	2	1	3	16.92	20.45	14.43	10.51	7.75
	3	1	2	23 98			4.99	

The magnetic symmetry groups compatible with the *Pnma* symmetry are well known to consist of eight possible configurations corresponding to the eight irreducible representations of *Pnma* for the propagation vector $k = (0, 0, 0)$. For the case of Mn atoms located in a symmetry centre, there are only four active representations (Bertaut 1963) (table 6). By inspection of table 5 one can see that all the reflections could be indexed with *hkl*, where $h+l = 2n+1$, and $k = 2n+1$. These are the selection rules for a magnetic G structure; i.e.,

Table 6. Crystallographic data of NH_4MnF_3 at 20 K. Space group *Pnma*, $Z = 4$ and the same crystallographic positions and choice of type of thermal parameters as in the refinement at 80 K (table 4). The magnetic moments of Mn are numbered M_1 at position 0 0 0, M_2 at position $0\frac{1}{2}0$, M_3 at position $\frac{1}{2}\frac{1}{2}\frac{1}{2}$ and M_4 at position $\frac{1}{2}0\frac{1}{2}$. Active representations: $\Gamma_1(+\,+\,+)$, $\Gamma_2(+\,-\,+)$, $\Gamma_3(-\,+\,+)$, $\Gamma_4(-\,-\,+)$ (signs refer to the parity under 2_{1x}, 2_{1z} and inversion operations on the magnetic moments). Magnetic modes: $F = M_1 + M_2 + M_3 + M_4$, $A = M_1 - M_2 - M_3 + M_4$, $C = M_1 + M_2 - M_3 - M_4$, $G = M_1 - M_2 + M_3 - M_4$. The magnetic structure is antiferromagnetic of G type with the magnetic moment, M, along the crystallographic b axis (mode G_y), $R_w = 6.7\%$, $R = 7.4\%$. The symbols Hk, m_i and s_i are defined in table 4 and in the text.

Atom	Position	x	y	z	Occupation	$\langle U \rangle$ (Å^2)
Mn	4a	0	0	0	4	0.0115(21)
N	4c	0.5000	$\frac{1}{4}$	0.0000	4	0.011
F1	8d	0.2720(17)	0.0084(18)	0.7675(20)	8	0.018
F2	4c	−0.0114(45)	$\frac{1}{4}$	0.0096(37)	4	0.018
H1	4c	−0.0442(37)	$\frac{1}{4}$	0.3348(47)	4.16(27)	0.029
H3	4c	0.1656(71)	$\frac{1}{4}$	0.5284(75)	4.15(27)	0.080
H8	8d	−0.0651(29)	0.3555(23)	0.5770(21)	7.84(49)	0.051

$M = 3.6(2)\mu_B$
$m_1 = 0.752(31)$
$m_2 = 0.248(31)$
$s_1 = 0.980(60)$
$s_2 = 0.000(28)$
$s_3 = s_2$
$s_4 = 0.061(39)$
$s_5 = 0.000(23)$
$s_6 = 0.056(43)$

where each magnetic moment has six nearest neighbours with their moments antiparallel to the first one.

In order to determine the alignment direction of the magnetic moment, we have calculated the intensities for the three orthorhombic directions, assuming a magnetic moment $M = 4\mu_B$ and two types of twinning domain identically populated. We can state that the alignment direction is the y axis, since the sequence of relative intensities in table 5 (No1 > No3 > No5 > No2 ≈ No4 > No7 ≈ No8 > No6) corresponds, within the uncertainty of the low intensity reflections, to the predicted one for G_y (No1 > No3 > No5 > No4 ≈ No8 ≈ No2 > No7 > No6). In contrast, it completely differs with respect to the sequence predicted for a G_x or G_z structure, where the predicted peaks for reflections hkl and lkh have been averaged (No1 > No2 > No3 > No4 > No5 ≈ No6 > No7 ≈ No8).

The previous qualitative analysis has led to the G_y magnetic structure. Now, the refinement of the atomic positions and the magnetic moment with the original 20 K data is performed using the described structure at 80 K for the starting atomic positions and thermal parameters: the results are shown in table 6. As far as the nuclear structure is concerned, only small variations of the parameters with respect to those at 80 K take place. The population of a single orientation of the NH_4^+ molecule and the structural domain subdivision is also corroborated at the lower temperature. The total magnetic moment obtained from the fit is $M = 3.6(2)\mu_B$, which is, within experimental error, similar to the value found in similar Mn perovskites, such as $KMnCl_3$ (Harris *et al* 1992).

No improvement in the fit is obtained if allowance is given for a ferromagnetic F_z or antiferromagnetic C_x component together with the antiferromagnetic one G_y. It should be recalled that all reflections derived from the ferromagnetic F_z component coincide with

those of the nuclear diffraction. If a canted magnetic component is present, it should be very small, but it cannot be evidenced by this ND work. In fact, other studies by ND on single crystals performed on distorted Mn perovskites, $KMnF_3$ (Hidaka *et al* 1975) or $KMnCl_3$ (Harris *et al* 1992), could not discern the existence of the canted moment. Only from complementary magnetic measurements could the weak ferromagnetism character be proved and the canting angle deduced. This is also our case, since from AC susceptibility data it could be proved that this compound has a weak ferromagnetic character below T_N, and from magnetization versus field measurements at 4.2 K the spontaneous magnetization of the canted moment could be measured, arriving at the conclusion that the canting angle was less than 0.1° (Bartolomé *et al* 1983).

Acknowledgments

This work has been supported by the CICYT project PB92-1077. The hospitality of ILL and CNRS in Grenoble is gratefully acknowledged. We thank M Le Blanc (Laboratoire des Fluorures, Université du Maine) for providing the single crystal of NH_4MnF_3.

References

Bartolomé J, Burriel R, Palacio F, Gonzalez D, Navarro R, Rojo J A and de Jongh L J 1983 *Physica* B **115** 190–204

Bartolomé J, Navarro R, Gonzalez D and de Jongh L J 1977 *Physica* B **92** 23–44

Bartolomé J, Palacio F, Calleja J M, Agulló-Rueda F, Cardona M and Migoni R 1985 *J. Phys. C: Solid State Phys.* **18** 6083

Bertaut E F 1963 *Spin Configurations of Ionic Structures: Theory and Practice* vol III, ed G T Rado and H Suhl (New York: Academic) p 149

Brückel Th, Prandl W, Vogt K and Zeyen C M E 1984 *J. Phys. C: Solid State Phys.* **17** 4071

Burriel R, Bartolomé J, Navarro R and Gonzalez D 1984 *Ferroelectrics* **54** 253–6

Fayos J 1990 *J. Phys. Chem. Solids* **51** 177–80

Harris P, Larsen S and Lebech B 1992 *J. Phys. Chem. Solids* **53** 1021–5

Helmholdt R B, Wiegers G A and Bartolomé J 1980 *J. Phys. C: Solid State Phys.* **13** 5081–8

Hidaka M, Oharna N, Okazaki A, Sakashita H and Yamakawa S 1975 *Solid State Physics* vol 16 (New York: Academic) pp 1121–4

Knop O, Oxton I A, Westerhaus W J and Falk M 1981 *J. Chem. Soc. Faraday Trans.* II **77** 309

Laguna M A, Sanjuán M L, Orera V M, Rubín J, Palacios E, Piqué M C, Bartolomé J and Berar J F 1993 *J. Phys.: Condens. Matter* **5** 283–300

Le Bail A, Fourquet J L, Rubín J, Palacios E and Bartolomé J 1990 *Physica* B **162** 231

Lundgren J O 1978 Uppsala University

Müller W and Hüller A 1982 *J. Phys. C: Solid State Phys.* **15** 7295

Navarro R, Burriel R, Bartolomé J and Gonzalez D 1987 *J. Chem. Therm.* **19** 579–94

Palacios E, Bartolomé J, Burriel R and Brom H B 1989 *J. Phys.: Condens. Matter* **1** 1119

Press W 1973 *Acta Crystallogr.* A **29** 257

Press W and Hüller A 1973 *Acta Crystallogr.* A **29** 252

Rubín J, Bartolomé J, Anne M, Kearley G J and Magerl A 1994a *J. Phys.: Condens. Matter* **6** 8449–68

Rubín J, Bartolomé J, Laguna M A, Sanjuán M L and Tompkinson J 1994b *J. Phys.: Condens. Matter* submitted

Smith D 1979 *Chem. Phys. Lett.* **66** 84–7

—— 1985 *J. Chem. Phys.* **82** 5133

—— 1987 *J. Chem. Phys.* **86** 4055

Vogt K and Prandl W 1983 *J. Phys. C: Solid State Phys.* **16** 4753